Fiber optical parametric chirped-pulse amplification in the femtosecond regime

Marc Hanna, Frédéric Druon, Patrick Georges

Fiber optical parametric chirped-pulse amplification in the femtosecond regime

Marc Hanna, Frédéric Druon, Patrick Georges

Laboratoire Charles Fabry de l'Institut d'Optique, Unité Mixte de Recherche 8501, Centre scientifique bât. 503, 91403 Orsay, France

marc.hanna@iota.u-psud.fr

Abstract: We study parametric amplification in optical fibers for chirped-pulse femtosecond laser systems. Compared to conventional OPCPA operating in bulk crystals, the fiber geometry offers a greater interaction length and spatial confinement, an increased flexibility in the choice of wavelengths for signal and pump beams, and the robustness of fiber setups. As opposed to rare-earth doped fibers, parametric amplifiers potentially provide wideband amplification in arbitrary regions of the spectrum. Numerical simulations are undertaken as a proof of principle for a picosecond 1064 nm pump and femtosecond 1025 nm signal. Guidelines for phase matching engineering are given, and limitations in spectral bandwidth and achievable pulse energy are discussed.

OCIS codes: (060.4370) Nonlinear optics, fibers; (190.4970) Parametric oscillators and amplifiers; (320.7140) Ultrafast processes in fibers.

References and links

1. N. Ishii, L. Turi, V. S. Yakovlev, T. Fuji, F. Krausz, A. Baltuska, R. Butkus, G. Veitas, V. Smilgevicius, R. Danielus, and A. Piskarskas, "Multimillijoule chirped parametric amplification of few-cycle pulses," Opt. Lett. **30,** 567–569 (2005).
2. J. V. Rudd, R. J. Law, T. S. Luk, and S. M. Cameron, "High-power optical parametric chirped-pulse amplifier system with a 1.55 μm signal and a 1.064 μm pump," Opt. Lett. **30,** 1974–1976 (2005).
3. I. Jovanovic, C. G. Brown, C. A. Ebbers, C. P. J. Barty, N. Forget, and C. Le Blanc, "Generation of high-contrast millijoule pulses by optical parametric chirped-pulse amplification in periodically poled $KTiOPO_4$," Opt. Lett. **30,** 1036–1038 (2005).
4. J. Hansryd, P. A. Andrekson, M. Westlund, J. Lie, and P.-O. Hedekvist, "Fiber-based optical parametric amplifiers and their applications," IEEE J. Sel. Top. Quantum Electron. **8,** 506–520 (2002).
5. A. Durecu-Legrand, A. Mussot, C. Simonneau, D. Bayart, T. Sylvestre, E. Lantz, H. Maillotte, "Impact of pump phase modulation on system performance of fibre-optical parametric amplifiers," Electron. Lett. **41,** 350–352 (2005).
6. G. K. L. Wong, A. Y. H. Chen, S. G. Murdoch, R. Leonhardt, J. D. Harvey, N. Y. Joly, J. C. Knight, W. J. Wadsworth, and P. St. J. Russell, "Continuous-wave tunable optical parametric generation in a photonic-crystal fiber," J. Opt. Soc. Am. B **22,** 2505-2511 (2005).
7. G. P. Agrawal, "Nonlinear fiber optics, " second edition, p. 49 and p. 428 (Academic Press, 1995).
8. M. E. Marhic, N. Kagi, T.-K. Chiang, and L. G. Kazovsky, "Broadband fiber optical parametric amplifiers," Opt. Lett. **21,** 573–575 (1996).
9. S. Fvrier, R. Jamier, J.-M. Blondy, S. L. Semjonov, M. E. Likhachev, M. M. Bubnov, E. M. Dianov, V. F. Khopin, M. Y. Salganskii, A. N. Guryanov, "Low Loss Large Mode Area Bragg Fibre," 31th European Conference on Optical Communication, Post Deadline paper PD Th4.4.3, Glasgow, United-Kingdom, 25-29 September 2005.
10. J. Marcou, F. Brchet, Ph. Roy, "Design of weakly guiding Bragg fibres for chromatic dispersion shifting towards short wavelengths," Journal of Optics A: Pure and Applied Optics **3,** S144-S153 (2001).
11. C. J. McKinstrie, S. Radic, and A. R. Chraplyvy, "Parametric amplifiers driven by two pump waves," IEEE J. Sel. Top. Quantum Electron. **8,** 538–547 (2002).

1. Introduction

Optical parametric chirped-pulse amplification (OPCPA) is recognized as a key technique to amplify ultrafast laser pulses. Its advantages over other CPA techniques include a broad bandwidth, good thermal properties, and access to arbitrary wavelength ranges. Recently, OPCPA has been successfully used to amplify few-cycle pulses [1] to multimillijoule energies, and to produce high-power pulses at 1.55μm [2]. Moreover, limitations due to the need of a phase-matching geometry can be overcome by periodically poling the amplifying medium [3]. These applications make use of the second-order nonlinearity of crystals.

Optical parametric amplification can also be performed in fibers, using the third-order nonlinearity of silica [4]. Intense research is conducted in this area for telecommunications applications, driven by the potential bandwidth and flexibility of this type of amplifiers. However, severe limitations have prevented the use of such amplifiers in commercial transmission systems. First, the gain flatness in a wavelength-multiplexed system must be on the order of a few dB, and even less in long-distance links. This is difficult to realize with parametric amplifiers. Second, because continuous-time amplification is needed in telecommunications, Brillouin scattering limits the pump power that can be launched in the fiber. Phase modulation of the pump can be used to overcome the latter problem, but noise transfer problems arise in this case [5]. Furthermore, it is not clear how new modulation formats using the optical phase will behave in the presence of this pump spectrum broadening scheme.

For both second- and third-order nonlinearity parametric amplification, energy conservation and phase-matching considerations determine the operating conditions. In crystals, this implies that the pump wavelength be shorter than the signal and idler wavelength. Phase-matching can be achieved using the birefringence of the crystal in conjunction with angle or temperature tuning. In fibers, the signal and idler wavelength are symmetric with respect to the pump in the case of single-wavelength pumping. The phase-matching condition is solely determined by the optical powers involved in the process and the fiber parameters, i. e. chromatic dispersion and nonlinear coefficient. The design of efficient parametric amplifiers therefore relies on the control of the dispersion curve and nonlinearity of fibers. Typically, the pump wavelength must be chosen in the zero group-velocity dispersion region.

Microstructured fibers allow such a control of the dispersion characteristics, opening up a wide field of possibilities for fiber-based parametric interactions [6]. In particular, fibers with zero group-velocity dispersion in the near infrared are now available, where ultrafast lasers based on Ti:Sapphire and Yb-doped crystals or fiber operate. We propose for the first time to our knowledge the use of optical fibers for femtosecond OPCPA systems and validate the idea with numerical simulations. The aforementioned drawbacks observed in fiber parametric amplifiers for telecommunication applications are avoided in femtosecond fiber OPCPA: the pump is pulsed, raising the Brillouin threshold, and the required gain flatness is less stringent than in WDM applications. First, numerical simulations are performed in the case of a femtosecond Yb laser at 1025 nm amplified by picosecond pulses from a typical Nd laser at 1064 nm with a commercially available fiber. These results establish the feasibility of fiber OPCPA with available technology. We then discuss the phase matching techniques and pulse energy limitations of this amplifying scheme, and suggest design rules for fibers that might be specifically designed for this application. An example of fiber design that could be used to amplify 70 fs-pulses is given to illustrate the potential of this technique.

2. Simulations

We first examine the use of a fiber OPCPA to transfer the high powers available in the ps regime for Nd lasers at 1064 nm to Yb-based femtosecond lasers at 1025 nm. This configuration is only possible for third-order nonlinearity based OPCPA because it allows the use of a pump

wavelength longer than the signal wavelength. The pump pulses are Gaussian, with a 40 ps full-width at half maximum (FWHM), and 1 kW peak power, corresponding to a 40 nJ energy. The signal pulses are 50 W peak-power 200 fs Gaussian pulses (10 pJ energy) stretched to 4 ps with a second-order dispersion of $\beta_2 z = 0.3$ ps^2 and third-order dispersion of $\beta_3 z = 3 \times 10^{-4}$ ps^3. The amplifying fiber zero-dispersion wavelength is 1040 nm ($\beta_2 = -3.0 \times 10^{-3}$ ps^2.m^{-1} at 1064 nm), with a dispersion slope of 0.2 ps/nm^2/km ($\beta_3 = 7.5 \times 10^{-5}$ ps^3.m^{-1} at 1064 nm), and an effective area of 18 μm^2, resulting in a nonlinear parameter $\gamma = 9.8$ W^{-1}.km^{-1}. These specifications correspond to the commercially available fiber Crystal Fibre NL-4.8-1040. Since it is difficult to evaluate from the supplier data, the derivative of the dispersion slope with respect to wavelength is taken equal to zero in the first simulation. It is then optimized for bandwidth in section 3. The propagation is modeled using an extended version of the nonlinear Schrödinger equation including Raman, self steepening, and dispersion effects up to fourth order:

$$\frac{\partial u}{\partial z} - j \sum_{k=2,3,4} \frac{j^k \beta_k}{k!} \frac{\partial^k u}{\partial t^k} = j\gamma \left(1 + \frac{j}{\omega_0} \frac{\partial}{\partial t}\right) \left[u(z,t) \int_{-\infty}^{t} R(t') |u(z,t-t')|^2 \, dt' \right] , \qquad (1)$$

where u is the electric field envelope, ω_0 is the central angular frequency, and $R(t) = (1 - f_R)\delta(t) + f_R h_R(t)$, where $f_R = 0.18$, is the normalized nonlinear response function. A commonly used analytic approximation was made for the shape of $h_R(t)$ [7]. The time, frequency and space sampling was checked to ensure accurate simulation results.

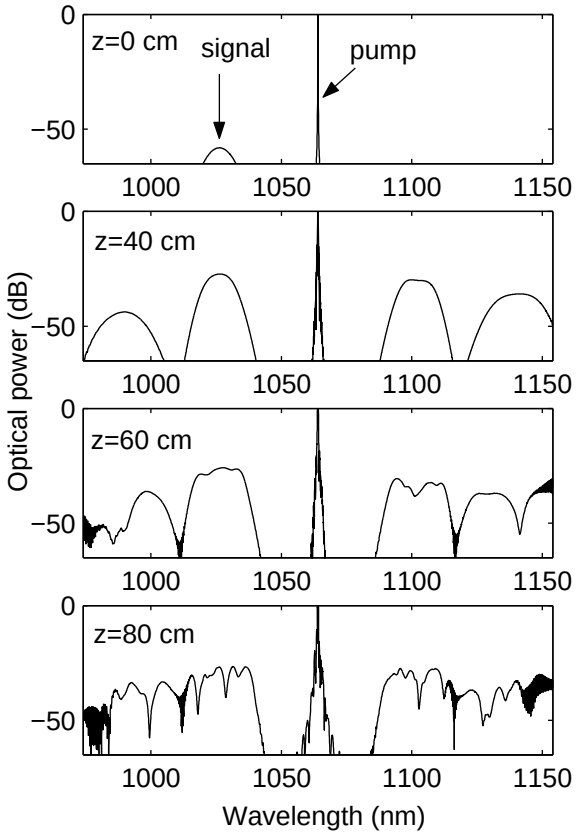

Fig. 1. Optical spectra at the input (top) and at various locations along the fiber.

Figure 1 shows the spectra at the input and along the fiber. At z=40 cm, the pulse at 1025 nm is clearly amplified and an idler wave at 1103 nm is created. We observe self-phase modulation of the pump, broadening its spectrum, but this will not be a limiting effect. The four wave-mixing process generates sidebands at shorter and longer wavelengths. For longer propagation distances, several parasitic nonlinear processes occur that degrade the quality of the amplified pulses. First, at z=60 cm, self-phase modulation of the signal and idler appear, broadening their spectra. Then a supercontinuum structure is created at z=80cm, drowning the signal. Indeed, the operating conditions, i. e. an intense pump pulse injected near the zero-dispersion wavelength of the fiber, are similar for supercontinuum generation. Efficient amplification therefore relies on a careful optimization of the parameters to favor amplification against competing nonlinear effects, mainly SPM. Although Raman and shock terms were included in the simulation, it appeared that they have little influence with the set of parameters used in this study. In this section, the amplifier output is now defined at z=40 cm.

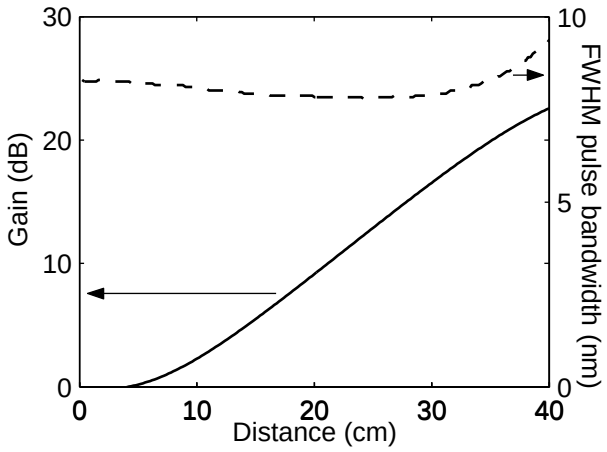

Fig. 2. Power gain (solid curve) and FWHM spectral width as a function of propagation distance in the fiber.

The evolution of FWHM pulse bandwidth and gain as a function of propagating distance is shown on Fig. 2. The bandwidth decreases very slightly along the propagation, then increases at the end of the fiber because of the onset of self-phase modulation. The gain is exponential and reaches 22 dB at the output of the amplifier before saturating because of the competing nonlinear effects. The output signal pulse energy is 1.5 nJ, giving an energy efficiency of 3.75%. After appropriate filtering (a 6 THz-bandwidth rectangular filter was used in the simulation), the output pulse can be recompressed to 210 fs, indicating that no shape degradation occurred in the amplifier. The group-velocity walk off between pump and signal is on the order of 100 fs, which is negligible compared to the stretched pulse duration.

An estimate of the gain curve can be analytically calculated using a simple CW approach [7]. Figure 3 shows this gain curve for the set of parameters used in the simulation. This curve shows that the CW phase matching condition is not fully satisfied at 1025 nm. The nonlinear phase matching shifts the CW peak gain to 1016 nm. Values of the gain obtained in the femtosecond regime model are shown on the same graph. We observe that the agreement is very good for signal wavelengths close to the pump, but the phase-matching peak is closer and less pronounced than in the CW regime. This can be interpreted as follows: first, the spectral content of both signal and pump wash out the sharp features of the CW regime. The other main deviation from the CW case is that, because of the pulsed nature of the pump, the pump power

seen by the signal can vary along the pulse. The power variation modifies both the gain value and the nonlinear phase-matching condition, related to the shape of the gain curve. This variation is more sensitive far from the pump wavelength, in the exponential gain region, which explains the good agreement between CW and femtosecond regime in the vicinity of the pump wavelength.

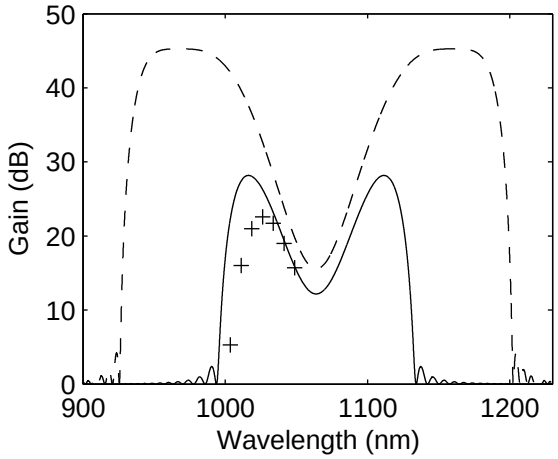

Fig. 3. Theoretical CW gain (solid line) and simulated fs-regime gain (crosses) of the fiber OPCPA described in section 2 as a function of wavelength. Theoretical CW gain (dashed line) corresponding to the bandwidth-optimized configuration described in section 3.

If the pump pulses are too short compared to the stretched pulse duration, the temporal wings of the signal pulse see less gain than the central part. Because the signal pulses are stretched, the temporal and spectral contents are closely related, and this translates into spectral gain narrowing over the entire bandwidth of the amplifier, thereby limiting the minimum duration of the pulses that can be amplified. Thus, special care must be taken in the choice of the pulsewidth ratio between stretched signal and pump in order to maximize the bandwidth. The use of long pump pulses also makes the amplifying scheme more tolerant to timing jitter between the pump and signal laser pulses. It is easily seen that this phenomenon is at the origin of a tradeoff between bandwidth and energy efficiency, as explained in further details in next section. In the ns regime, square pulse shaping on the pump can be used to relax this tradeoff. On the other hand, this effect can be used to tailor the spectral gain curve of the amplifier by changing the relative delay between pump and signal.

Despite these differences, general design rules obtained in the case of quasi-CW fiber PA based on the analytic expression of the gain given in [7] apply to fiber OPCPA : for a fixed nonlinear phase shift of the pump, the bandwidth of the amplifier increases with decreasing fiber length [4]. Also, fourth-order dispersion can be used to increase and flatten the bandwidth for a given β_2 [8]. An example of such an optimization of the phase matching is given in next section.

3. Energy and bandwidth limitations

We now discuss the energy limitations of this amplifying scheme. If we assume a lossless fiber and no pump depletion, the maximum nonlinear phase accumulated by the pump along the fiber is given by $\phi_p = \gamma P_p z$, where γ is the nonlinear coefficient of the fiber, P_p is the peak pump power, and z is the propagation distance. The value of the gain G varies over the band-

width of the amplifier, between a quadratic gain region in the vicinity of the pump wavelength and an exponential gain at the phase-matching wavelength. The dominant energy limitation comes from self-phase modulation on the signal that prevents proper recompression. Let us fix a maximum nonlinear phase value of ϕ_s on the signal. Empirically, we found that $\phi_s < 0.4$ ensures no degradation on the output pulses. This nonlinear phase shift can be evaluated as

$$\phi_s = \int_0^L \gamma P_s(z) dz = \gamma P_{eq} L \ , \tag{2}$$

where L is the length of the amplifier, $P_s(z)$ is the peak signal power along the amplifier, and P_{eq} depends on the type of gain : $P_{eq} = P_s(0)(G-1)/\ln(G)$ for exponential gain and $P_{eq} = P_s(0)G/3$ for quadratic gain. Replacing these expressions in the inequality that defines the maximum nonlinear phase shift, and defining the pulsewidth ratio between the stretched signal and pump R_{sp}, we obtain a limit on the signal to pump energy ratio at the input of the fiber E_s/E_p. In the exponential gain region, we find

$$\frac{E_s}{E_p} < \frac{\phi_s \ln(G) R_{sp}}{G\phi_p} \ , \tag{3}$$

while in the quadratic gain region, this ratio is given by

$$\frac{E_s}{E_p} < \frac{3\phi_s R_{sp}}{G\phi_p} \ . \tag{4}$$

These upper bounds can also be seen as limits on the energy efficiency defined as GE_s/E_p. In our example, it evaluates to 3.8%, in good agreement with numerical simulations that give an output pulse energy of 1.5 nJ. The relation between the pulsewidth ratio and energy efficiency clearly appears in these inequalities, leading to a tradeoff between energy efficiency and bandwidth. In our example, setting all parameters constant except for pump pulsewidth, the maximum energy efficiency was found to be 15%, corresponding to 10 ps pump pulses. In this case, slight gain narrowing led to a recompressed pulse duration of 230 fs. Further decrease of the pump pulse duration led to significant gain narrowing and longer recompressed pulses at the output.

To scale the output pulse energy to higher values while keeping the gain constant, one could use fibers with a broader mode area, thereby decreasing γ, while increasing the pump power or the length to compensate for the loss of efficiency in the interaction. However, for the type of fiber considered here, where guiding relies on total internal reflection between the silica core and the cladding essentially made of air, increasing the mode area translates into a modification of the dispersion properties. This in turn modifies the phase matching condition of the interaction, affecting the amplifier performance. Ultimately, for very large mode areas, the dispersion is essentially defined by the silica material, fixing the operation wavelength at 1.3 μm. A possible way to overcome this problem could be to use fibers where guiding is based on a photonic bandgap, such as Bragg fibers [9]. In such structures it is possible to shift the group-velocity dispersion towards short wavelengths [10].

To remain at fixed ϕ_p, it is preferable to increase the pump power because increasing the length leads to a reduced bandwidth of the amplifier. Depending on the repetition rate and peak power of the pump pulses, issues such as optical surface damage and thermal effects in fibers must be addressed when scaling the pump power. For instance, end-caps might be used to avoid surface damage at the facets of the fiber. Increasing the signal stretching ratio provides a convenient way to increase output pulse energy while keeping self-phase modulation at a tolerable level. Although we use a stretching ratio of 20 to facilitate the numerical simulations, values of the order of 10000 are commonplace in experimental CPA systems. We therefore

expect that $> \mu$J pulse energies are attainable using large-mode area fibers and longer stretched signal and pump pulses.

To illustrate the potential bandwidth of the fiber OPCPA scheme, an example of possible optimization is now presented based on the previous configuration. Following the analysis given in [8], we use fourth-order dispersion to enhance the bandwidth, along with a higher pump power and reduced fiber length. The parameters of the amplifier are the following: the effective area, second-, and third-order dispersion parameters are unchanged, fourth order dispersion is set to $\beta_4 = 7 \times 10^{-55}$ s^2.m^{-1} at 1064 nm, pump pulses are 40 ps long with a peak power of 2 kW, and the fiber length is reduced to 30 cm. These parameters result in a flat CW gain region extending from 940 to 1010 nm using a 3 dB cutoff criterion, as shown in fig. 3. The input signal pulses are 70-fs FWHM long, centered at 980 nm, with a peak power of 50 W, and are stretched with the same dispersion values as in the first simulation. Figure 4 shows the input and output spectra and waveform for this configuration. The gain in energy is 27 dB, producing 1.7 nJ ouput pulses. Four-wave mixing generates some spectral content on the short-wavelength side of the signal, which prevents from using a signal wavelength closer to the pump. The amplified spectrum exhibits a slight gain narrowing effect, with the FWHM spectral width being reduced from 34 nm down to 27 nm, consistent with a recompressed pulsewidth of 85 fs.

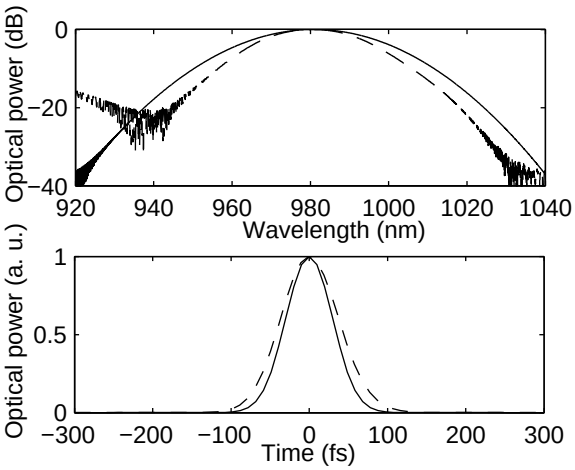

Fig. 4. Input (solid line) and output (dashed line) spectra (top) and waveforms (bottom) of the large bandwidth fiber OPCPA.

The fiber implementation of OPCPA also allows the use of the idler for optimal recompression. Since the idler and signal are phase-conjugated, an exact copy of the signal stretcher can be used to recompress the idler after amplification. In crystal-based OPCPA systems, the idler inherits spatial properties from the pump beam, which prevents its use if no special care is taken to address this problem. In fibers, however, the idler wavefront is determined by the waveguiding properties, ensuring a flat wavefront in singlemode fibers. Along with wavelength conversion, the use of the idler therefore allows potentially simple compressor implementation.

4. Conclusion

In summary we have proposed the use of optical fibers to fabricate OPCPA systems in the femtosecond regime. Numerical simulations show the feasibility of such a scheme in a typical configuration using a commercially available fiber. Many other wavelength configurations of interest are feasible, provided that fibers exhibiting the right dispersion and nonlinear charac-

teristics can be fabricated. Moreover, the other degrees of freedom available for design (pump power, fiber length) make this amplifier scheme very versatile. Configurations with a 1064 nm pump and 800 nm signal could be imagined. In the 1300 nm region, high power Nd-based pump lasers and conventional large mode area fibers exhibiting zero group-velocity dispersion are readily available, making another potential configuration. The design rules of CW parametric amplifiers should allow the engineering of microstructured fibers specially dedicated to OPCPA. For even more flexibility, two-pump schemes [11] could also be used to further extend the operating bandwidth.